Nanoscience and Nanotechnology 2016, 6(4): 62-67
DOI: 10.5923/j.nn.20160604.02

Simulation Investigations of Structural, Electronic, Optical and Elastic Properties of the $Cu_xTi_{1-x}O_2$

Yasaman Abed[1], Fatemeh Mostaghni[2,*]

[1]Physic Department, Payam Noor University, Iran
[2]Chemistry Department, Payam Noor University, Iran

Abstract In this study, the electronic, optical and elastic properties of Cu-dopped TiO_2 were theoretically investigated. The calculations have been performed using castep code in the framework of density functional theory with LDA and GGA approximations. Comparison between the experimental and the theoretical results indicates that the simulational method is able to provide satisfactory results for predicting the properties of the considered compounds. The best results were achieved by GGA+PBE approximation. It served as an additional proof of reliability of these theoretical findings and gave confidence in the results of the following calculations of the electronic, optical and elastic properties of Cu doped TiO_2 semiconductor.

Keywords Simulation, Electronic properties, Elastic constants, Semiconductor

1. Introduction

Among the inorganic oxide semiconductors, titanium dioxide is highly noteworthy due to its chemical stability, non-toxicity and low cost [1-5]. It is used in a wide range of fields, including pigments, solar energy transfer, photocatalyst and so on. Titanium dioxide exists in three crystalline phases includes rutile (cubic), anatase (tetragonal) and brookite (orthorhombic). Rutile, is the most stable phase of titanium dioxide in bulk and environmental conditions.

It should be noted that the production of titanium dioxide, affects the final phase of production [6-10]. The mechanism of all its characteristics includes lighting the surface of titanium dioxide with energies greater than its band gap and exciting electrons from valance band to conducting band [11]. However, the use of titanium dioxide has been limited by two reasons [12]:

1- The band gap of titanium dioxide is in the ultraviolet (UV), while less than 10% of sunlight is in the ultraviolet region of the spectrum.
2- Rapid pairing of electron-hole which results in the loss of photo-catalytic activity.

In recent years, the number of ways to modify titanium dioxide with metals and non-metals and sensitization of titanium dioxide have been used [13-15].

Different investigations show that doping of TiO_2 by low amounts of metals and nonmetals elements, sometimes leads to enhanced photocatalytic activity and to an increase of visible light absorption [16, 17].

Producing solar cells based on titanium dioxide is the new generation of photo-volta cells that regarding its low cost have been proposed as an alternative to the solar cells [18]. In the area of solar energy, doping with Cu element significantly extends the light absorbtion of TiO_2 into the visible region, which further enhance the photoelectro chemical properties of the TiO_2 [19].

The understanding of detailed electronic structure of semiconductors has been a challenging problem in electronics. Unfortunately, measurements of structure and electronic properties of crystals require a specified laboratory, as well as excellent quality materials, which is generally expensive. In contrast to experimental investigations, a theoretical analysis by computer simulations could overcome the effects of complex experimental factors and clarify the ion doping effects on crystal and electronic structure.

Quantum chemistry calculations of modifying the band gap of TiO_2 have been reported, including studies of transition metals co-doping of TiO_2 photocatalysts [20-23].

Yalc et al. performed calculations based on density functional theory (DFT) to characterize the influence of Fe^{3+} doping on the electronic and structural properties of TiO_2 [24]. Recently, first-principles calculations were conducted for Fe-doped TiO_2 [25-28].

In our previous study we have performed a careful and systematic analysis of the cobalt impurity states in different concentrations as well as their influence on the TiO_2 band structure and density of states [29].

* Corresponding author:
mostaghnif@yahoo.com (Fatemeh Mostaghni)
Published online at http://journal.sapub.org/nn

In this paper the electronic band structure, density of state, optical and elastic properties of Cupper doped TiO_2 nanocomposite simulated using castep code. Castep employs the first-principles density functional theory that explore the properties of crystals and surfaces in materials, such as, semiconductors, ceramics, metals, minerals and zeolites.

2. Materials and Methods

All presented calculations were performed using a first principle plane wave pseudo-potential technique based on density functional theory with CASTEP module [30] of Materials Studio. Calculations are performed with either generalized gradient (GGA) or the local density approximation (LDA) to treat the exchange–correlation effects. [31]. To obtain the desired accuracy, we selected 973 points in 6 × 6 × 7 K_point. Computations for TiO_2 crystal are done in anatase phase (141/amd space group) with lattice constant a = b = 3.7834 and c = 9.4841. The structural data from ref. [32] were taken as an initial input for all calculations.

3. Results and Discussion

3.1. Electeronic Properties

In this study Cu dopant is substituted into anatase structure in Ti lattice site in various concentrations (0, 1 and 2%). Then the electronic structures and band parameters of three samples are obtained using either generalized gradient (GGA) or the local density approximation (LDA). From the above simulations, it is found that the band structure and density of states of three samples are nearly same from the LDA and GGA. The band gap values for all samples is determined from the band structures and density of state, by two methods. The results are summarized in table 1.

Table 1. The band gap (eV) values calculated by LDA and GGA methods

sample	method		
	GGA	LDA	exp
TiO_2	2.14	2.09	3.04
Cu/TiO_2 (1%)	1.81	1.74	2.80
Cu/TiO_2 (2%)	1.94	1.92	2.83

It can be observed that the values of bond gap complement the experimental findings and reported results. The best fittings between calculated and measured band gap were achieved by GGA aproximation. With this level, the deviations between calculated and experimental values are smaller than LDA methods. It serves as an additional proof of reliability of these theoretical findings and gives confidence in the results of the following calculations of the electronic, optical and elastic properties which presented in the next sections.

The calculated band structures of pure and Cu doped TiO_2 are shown in figure 1. The fermi level is chosen to be zero of the energy scale. As we can see, the band structure of pure anatase TiO_2 shows semiconducting behavior, because in this case indirect energy band gap is 2.14 eV. It is less than the experimental value E_g = 3.04 eV. This underestimation is an intrinsic feature of the density functional theory.

Figure 1a shows that the top of valence bands (VBs) appears to be relatively flat and the bottom of conduction bands (CBs) have small dispersion. Figure 1b and 1c shows the substitution of Cu dopant created impurity states in electronic band structure of anatase. The Cu introduced two lone pair states just above to the valence band maximum thus reduced the band gap of TiO_2 with an optimal doping concentration of 1 %.

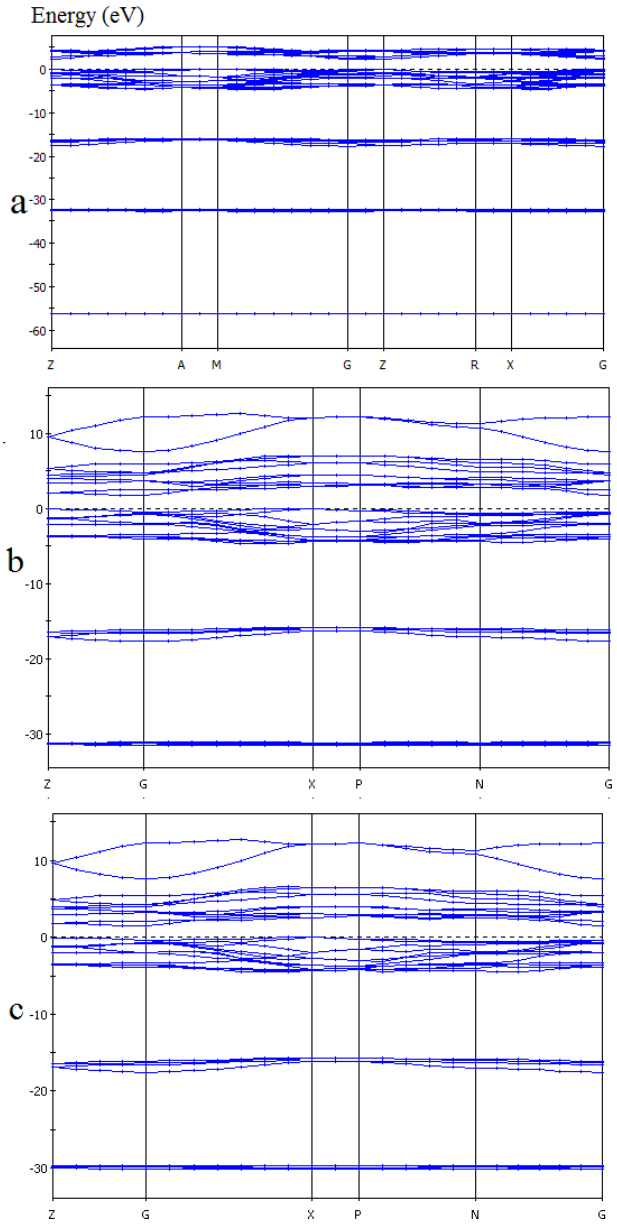

Figure 1. Band structure and of $CuxTi_{1-x}O_2$ for (a) x= 0%, (b) 1% and (c) 2% in GGA method

The DOS of pure and Cu doped TiO_2 are also shown in figure 2. In figure 2a, we can also clearly see the conduction bands, are mostly formed by Ti-4d state, with a contribution of the O-3p states. While the valance bands are mainly consist of the hybridizations of Ti-3d states and O-2p states. In figure 2b and 2c it can be observed that the source of energy is also located in the maximum capacity band with conductive bands on top where overlap exists in 3d titanium and 4d cupper in an area that represents the overlap of 3d titanium and 4d cupper orbitals.

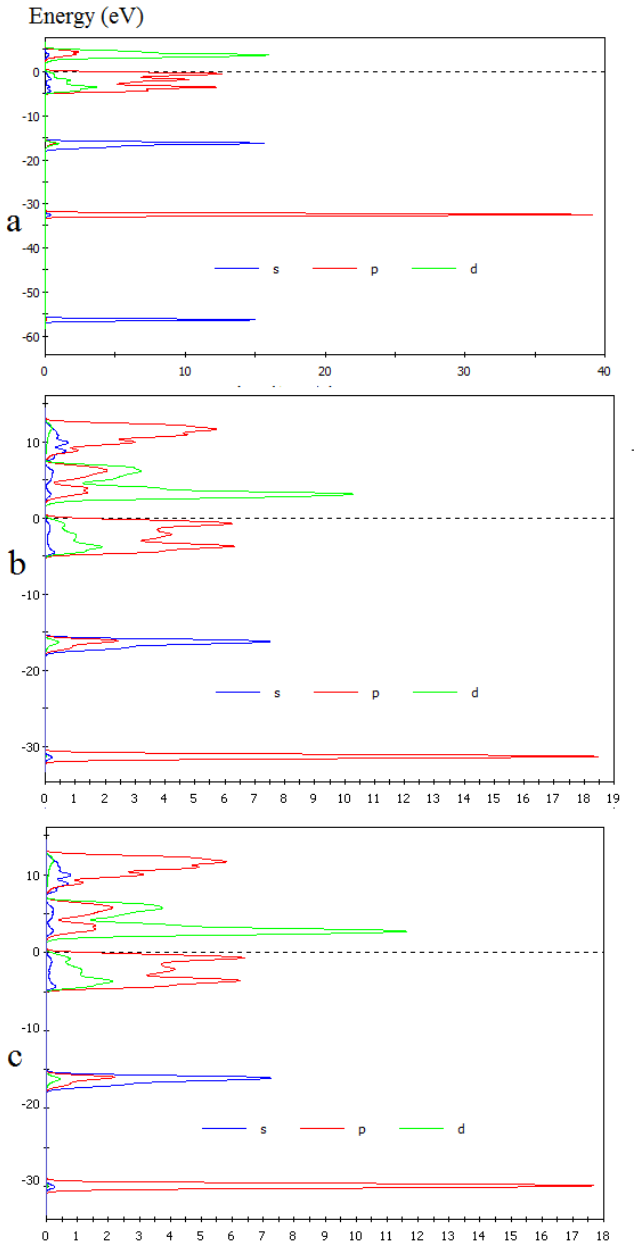

Figure 2. Density of state of $CuxTi_{1-x}O_2$ for (a) x= 0%, (b) 1% and (c) 2% in GGA method

3.2. Optical Properties

The optical properties of matter can be described through the complex dielectric function ε(ω) as following [33]:

$$\varepsilon(\omega) = \varepsilon_1(\omega) + i\varepsilon_2(\omega)$$

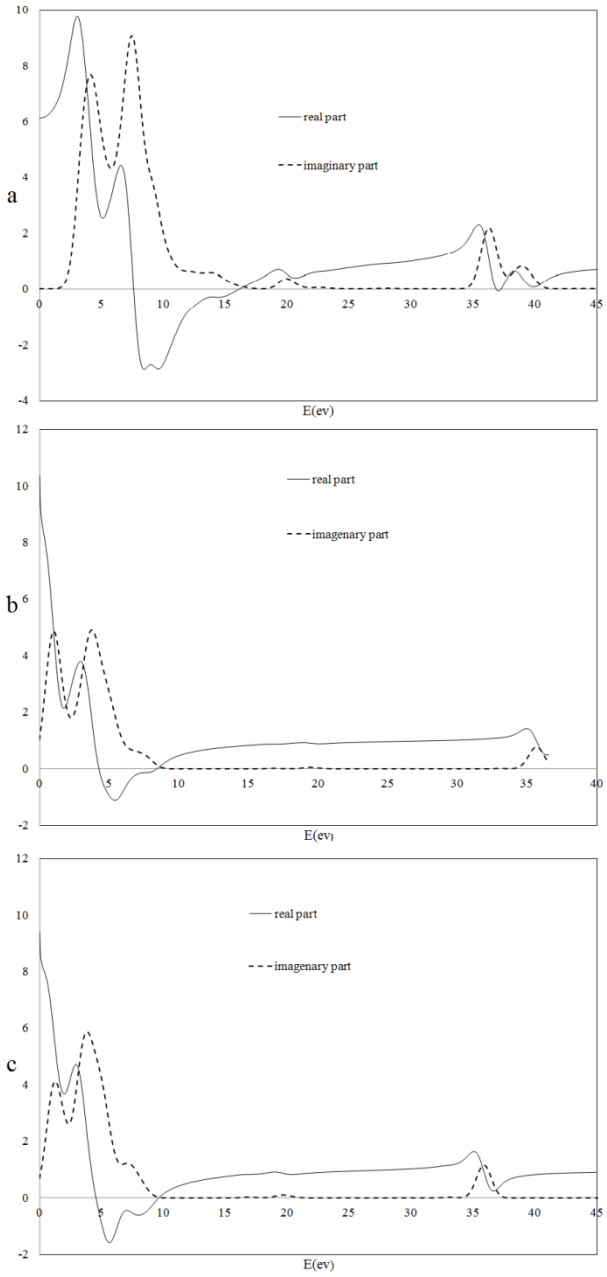

Figure 3. The imaginary part of dielectric function for $Cu_xTi_{1-x}O_2$ for (a) x= 0% , (b) 1% and (c) 2%

The imaginary part of the dielectric function $\varepsilon_2(\omega)$ is associated with the dissipation and as a consequence, it is responsible for the absorption. It is well known that the interaction of a photon with the electrons in the system can be defined in terms of time-dependent perturbations of the ground-state electronic states. If an incoming photon can couple a filled state to an empty state, there will be absorption. If there are a lot of photons which can couple these two states, there will be a big peak in the imaginary part of the dielectric function, because there will be more absorption.

The $\varepsilon_2(\omega)$ is obtained from the momentum matrix

elements between the occupied and the unoccupied electronic states and calculated directly by [34]:

$$\mathrm{Im}\epsilon_{\alpha\beta}(\omega) = \frac{4\pi e^2}{m^2\omega^2}\sum_{cy}\int_0^{\infty}\langle C_k|P^{\alpha}|\vartheta_K\rangle\langle\vartheta_k|P^{\beta}|C_K\rangle\delta$$
$$(\varepsilon_{ck} - \varepsilon_{\vartheta k} - \omega)dK$$

Where e is the electronic charge, C_k and υk are the conduction and valance band wave function at k respectively, and ω is the light frequency.

The imaginary part calculations of the dielectric function for $Cu_xTi_{1-x}O_2$ for x = 0, 1 and 2% are shown in Figure 3.

We observe that the values of $\varepsilon_2(\omega)$ for all the binary and ternary alloys are naturally shifted towards lower energies with the amplitude increasing as increases Cu concentration. This confirm our results that the increase in Cu concentration causes a decrease in indirect band gap.

The real part of the dielectric function can be calculated by the Kramer-Kronig relation as bellow [35]:

$$\mathrm{Re}\epsilon_{\alpha\beta}(\omega) = \delta_{\alpha\beta} + \frac{2}{\pi}P\int_0^{\infty}\frac{\omega\mathrm{Im}\acute{\varepsilon}_{\alpha\beta(\acute{\omega})}}{\acute{\omega}^2 - \omega^2}d\acute{\omega}$$

where P is the Kooshy integral section.

The present results of calculated $\varepsilon_1(\omega)$ are shown in Figure 3. An important quantity of $\varepsilon_1(\omega)$ is the zero frequency limit $\varepsilon_1(0)$. It represents the dielectric response to the static electric field, which is the electronic part of the static dielectric constant and strongly depends on the band gap.

In $Cu_xTi_{1-x}O_2$, value of $\varepsilon_1(0)$ increases from 6.14 to 10.37 and the direct band gap decreases With increasing the Cu concentration.

3.3. Elastic Properties

The elastic constants of solids provide a link between the mechanical and dynamical behaviours of crystals. In the present work, we performed systematic first-principles calculations of the elastic constants C_{ij} (Table 2), bulk moduli B, compressibility K, shear moduli G, Young's moduli Y and the Poisson ratio v for $Cu_xTi_{1-x}O_2$ (Table 3).

Table 2. Calculated elastic C_{ij}

Compound	C_{11}	C_{33}	C_{44}	C_{66}	C_{12}	C_{13}
TiO_2	302.840	153.887	68.102	47.729	70.503	51.164
Cu/TiO_2 (1%)	278.469	167.813	42.714	45.664	92.090	62.271
Cu/TiO_2 (2%)	279.129	181.756	21.211	43.229	95.174	63.488

Table 3. Calculated elastic parameters for $Cu_xTi_{1-x}O_2$

Compound	B (GPa)	K (1/GPa)	G (GPa)	Y (GPa)	ν
TiO_2	109.5940	0.00912	72.18007	177.55	0.229
Cu/TiO_2 (1%)	119.07499	0.0084	56.74557	146.88	0.294
Cu/TiO_2 (2%)	122.5966	0.00816	43.71230	117.20	0.34

Values of E and σ are computed using the following relationships [36].

$$E = \frac{9BG}{3B + G} \quad \text{and} \quad \sigma = \frac{3B - 2G}{2(3B + G)}$$

The calculated six independent elastic coefficients for each doping level were found to be positive and satisfy the known born criterion for a mechanically stable system: $(C_{11}+ C_{33}- 2C_{13}) > 0$ $C_{11}> 0$, $C_{33}> 0$, $C_{44}> 0$, $C_{66} > 0$, $[2(C_{11}+ C_{12}) + C_{33}+ 4C_{13}] > 0$ and $(C_{11}- C_{12}) > 0$). To define true polycrystalline constants, the values for their upper and lower limits were given by Hill. He showed polycrystalline moduli in terms of voigt and reuss approximation, and are given by [37].

Hill's shear modulus:

$$G_H \equiv G = 1/2(G_R + G_V)$$

Hill's bulk modulus:

$$B_H \equiv B = 1/2(B_R + B_V)$$

Where B_R and B_v are the reuss's and voigt's bulk modulus and G_R and G_v are the reuss's and voigt's shear modulus, respectively.

From our calculations, it is found that the $Cu_xTi_{1-x}O_2$ is stiffer than the pure anatase TiO_2, because the balk modul of Cu/TiO_2 was bigger than pure TiO_2. The Poisson's ratio (σ) takes the value: $0 < \sigma < ½$. The lower limit and upper limit for central forces in solids are $\sigma = 0.25$ and $\sigma = 0.5$ respectively. The present calculated result showed that poisson's ratio (σ) of TiO_2 and $Cu_xTi_{1-x}O_2$ was larger than the lower limit value ($\sigma = 0.25$), which indicates that the interatomic forces of $Cu_xTi_{1-x}O_2$ are central forces.

4. Conclusions

Calculations based on density functional theory have been carried out. The calculated values are in good agreement with experimental results and few conflicts are due to density function failure. The results show that by increasing Cu, the energy gap decreases and finally dielectric constant will increase which satisfy the corresponding experimental data result.

The Cu introduced two lone pair states just above to the valence band maximum. Therefore charge transfer (CT) processes from the TiO_2 valence band to Cu(II) and from Cu(II) to the conduction band Occur upon visible light. In other word Cu doping reduced the band gap of TiO_2 with an optimal doping concentration of 1 %. The best results were achieved by GGA+PBE approximation. In addition, it is found that the $Cu_xTi_{1-x}O_2$ is stiffer than the pure anatase TiO_2, because the balk modul of Cu/TiO_2 was bigger than pure TiO_2. In the area of solar energy, doping with Cu element that significantly extends the light absorbtion of TiO_2 into the visible region, further enhance the photoelectro chemical properties of the TiO_2.

ACKNOWLEDGEMENTS

We would like to thank Fars Payam Noor University for their support and encouragements.

REFERENCES

[1] Colmenares, J. C., Aramendia, M. A., Marinas, A., Marinas, J. M., Urbano, F. J., 2006, Synthesis, Characterization and Photocatalytic Activity of Different Metal-Doped Titania Systems, Applied Catalysis A, 306, 120-127.

[2] Crisan, M., Braileanu, A., Raileanu, M., Zaharescu, M., Crisan, D., Dragan, N., Anastasescu, M., Ianculescu, A., Nitoi, I., Marinescu, V. E., Hodorogea, S. M., 2008, Sol-gel S-doped TiO_2 materials for environmental protection, Journal of Non-Crystalline Solids, 354, 705-711.

[3] Ding, X., An, T., Li, G., Zhang, S., Chen, J., Yuan, J., Zhao, H., Chen, H., Sheng, G., Fu, J., 2008, Preparation and characterization of hydrophobic TiO_2 pillared clay: the effect of acid hydrolysis catalyst and doped Pt amount on photocatalytic activity, Journal of Colloid and Interface Science, 320 (2), 501-507.

[4] Chen, S.L., Wang, A.J., Dai, C., Benziger, J.B., Liu, X.C. 2014, The Effect of Photonic Band Gap on the Photocatalytic Activity of nc-TiO_2/SnO_2 Photonic Crystal Composite Membranes, Chemical Engineering Journal, 249(1), 48-53.

[5] Kato, H, Kudo, A, 2002, Visible-Light-Response and Photocatalytic Activities of TiO_2 and $SrTiO_3$ Photocatalysts Codoped with Antimony and Chromium. Journal of Physical Chemistry B, 106(19), 5029-5034.

[6] Mali, S.S., Betty, C.A., Bhosale, P.N., Patil, P.S., Hong, C.K. 2014, From Nanocorals to Nanorods to Nanoflowers Nanoarchitecture for Efficient Dye-sensitized Solar Cells at Relatively Low Film Thickness: All Hydrothermal Process, Scientific Reports, 4,1-8.

[7] Gao, Y., Masuda, Y., Seo, W.S., Ohta, H., Koumoto, K., 2004, TiO_2 nanoparticles prepared using an aqueous peroxotitanate solution, Ceramics International, 30, 1365-1368.

[8] Wu, M.C. Sápi, A., Avila, A., Szabó, M., Hiltunen, J., Huuhtanen, M., Tóth, G., Kukovecz, A., Kónya, A., Keiski, R., Su, W.F., Jantunen, H., Kordás, K., 2011, Enhanced photocatalytic activity of TiO_2 nanofibers and their flexible composite films: Decomposition of organic dyes and efficient H2 generation from ethanol-water mixtures, Nano Research, 4(4), 360-369.

[9] Yang, J., Mei, S., Ferreira, J.M.F., 2001, Hydrothermal synthesis of TiO_2 nanopowders from tetraalkylammonium hydroxide peptized sols, Materials Science and Engineering C, 15, 183-185.

[10] Yang, S., Liu, Y., Guo, Y., 2002, Preparation of rutile titania nanocrystals by liquid method at room temperature, Materials Chemistry and Physics, 77, 501-506.

[11] Bak, T., Li, W., Nowotny, J., Atanacio, A.J., Davis, J., 2015, Photocatalytic Properties of TiO_2: Evidence of the Key Role of Surface Active Sites in Water Oxidation, Journal of Physical Chemistry A, 119(36), 9465–9473.

[12] Pelaez, M., Nolan, N., Pillai, S., Seery, M., Falaras, P., Kontos, A., Dunlop, P., Hamilton, J., Byrne, J., Oshea, K., 2012, A review on the visible light active titanium dioxide photocatalysts for environmental applications, Applied Catalysis B, 125, 331–349.

[13] Mostaghni, F., Abed, Y., 2016, Structural, Optical and Photocatalytic Properties of Co-Tio_2 Prepared by Sol-Gel Technique, Materials Research, 19(4), 741-745.

[14] Komai, Y., Okitsu, K., Nishimura, R., Ohtsu, N., Miyamoto, G., Furuhara, T., Semboshi, S., Mizukoshi, Y., Masahashi, N., 2011, Visible Light Response of Nitrogen and Sulfur Co-Doped TiO_2 Photocatalysts Fabricated by Anodic Oxidation, Catalysis Today, 164, 399-403.

[15] Jia, X., Fan, H., Afzaal, M., Wu, X., Brien, P.O., 2011, Solid State Synthesis of Tin-Doped ZnO at Room Temperature: Characterization and Its Enhanced Gas Sensing and Photocatalytic Properties, Journal of Hazardous materials, 193, 194-199.

[16] Zhou, S., Lv, J., Guo, L.K., Xu, G.Q., Wang, D.M., Zheng, Z.X., Wu, Y.C., 2012, Preparation and Photocatalytic Properties of N-Doped NanoTiO_2/Muscovite Composites, Applied Surface Science, 258, 6136-6141.

[17] Collazzo, G.C., Foletto, E.L., Jahn, S. L., Villetti, M.A., Degradation of Direct Black 38 Dye under Visible Light and Sunlight Irradiation by N-Doped Anatase TiO_2 as Photocatalyst, Journal of Environmental Management, 98, 107-111.

[18] Bianco-Prevot, A., Baiocchi, C., Brussino, M.C., Pramauro, E., Savarino, P., Augugliaro, V., Marci, G., Palmisano, L. 2001, Photocatalytic degradation of Acid Blue 80 in aqueous solutions containing TiO_2 suspensions. Environmental Science and Technology, 35, 971-976.

[19] Liu, Y., Zhou, H., Li, J., Chen, H., Li, D., Zhou, B., Cai, W. 2010, Enhanced photoelectrochemical properties of Cu_2O-loaded short TiO_2 nanotube array electrode prepared by sonoelectrochemical deposition. Nano-Micro Letters, 2(4), 277-284.

[20] Zheng, L., Cheng, H., Liang, F., Shu, S., Tsang, C.K., Li, H., Lee, S., Li, Y., 2012, Porous TiO_2 Photonic Band Gap Materials by Anodization, Journal of Physical Chemistry C, 116(9), 5509–5515.

[21] Zheng S., Guohao, W., Zhang, G., Suoling, Z., Jie, S., Leil, L., Fang, W., Rui, Z., Xiaobing, Y., Material Science Poland, 32, 93.

[22] Karthik, K., Kesava, P., Pandian, S., Suresh, K., 2010, Influence of dopant level on structural, optical and magnetic properties of Co-doped anatase TiO_2 nanoparticles, Journal of Applied Surface Science, 256, 4757-4760.

[23] Li, H., Chen, L., Liu, S., Li, C., Meng, J., Wang, Z., Yoon, J., Shim, E., Joo, H., 2009, First-principles study of atomic structure and electronic properties of Si and F doped anatase TiO_2, Journal of Chemical Engineering, 26, 1296.

[24] Li, H., Chen, L., Liu, S., Li, C., Meng, J., Wang, Z., 2015, First-principles study of atomic structure and electronic properties of Si and F doped anatase TiO_2, Materials Science-Poland, 33(3), 549–554.

[25] Kapilashrami, M., Zhang, Y., Liu, Y.S., Hagfeldt, A., Guo, G.,

2014, Probing the Optical Property and Electronic Structure of TiO_2 Nanomaterials for Renewable Energy Applications, Chemical Reviews, 114(19), 9662-9707.

[26] Hou, X.G., Huang, M.D., Wu, X.L., Liu, A., 2009, First-principles calculations on implanted TiO_2 by 3d transition metal ions, Science China Physics, Mechanics & Astronomy, 52, 838-842.

[27] Su, Y., Xiao, Y., Li, Y., Du, Y., Zhang, Y., 2011, Preparation, photocatalytic performance and electronic structures of visible-light-driven Fe–N-codoped TiO_2 nanoparticles, Materials Chemistry and Physics, 126 (3), 761-768.

[28] Jia, l., Wu, C., Han, S., Yao, N., Li, Y., Li, Z., Chi, B., Pu, J., Jian, L., 2011, Theoretical study on the electronic and optical properties of (N, Fe)-codoped anatase TiO_2 photocatalyst, Journal of Alloys and Compounds, 509(20), 6067-6071.

[29] Mostaghni, F., Abed, Y., 2015, First-Principles Study on Anatase Co/TiO_2: Effect of Co Concentration, Physical Chemistry, 5(2), 34-38

[30] Clerk, S.J., Segall, M.D., Pickard, C.J., Hasnip, P.J., Probert, M.I.J., Refson, K., Payne, M.C. Z. 2005, First principles methods using CASTEP. Z. Kristallogr. 220, 567-570.

[31] Cottenier, S. 2002, Density Functional Theory and the family of (L) APW-methods: a step-by-step introduction. Belgium, Instituut voor Kernen Stralingsfysica, K.U. Leuven.

[32] Langreth, D.C., Perdew, J.P. 1980, Theory of nonuniform electronic systems. I. Analysis of the gradient approximation and a generalization that works. Physical Review B: Condensed Matter, 21, 5469-5493.

[33] Amrosch-Draxl, C., Sofo, J.O. 2006, Linear optical properties of solids within the full-potential linearized augmented planewave method. Computer Physics Communications, 175(1), 1-14.

[34] Ivanovskii, A.L. 2009, New superconductors based on (Ca, Sr, Ba) Fe_2As_2 ternary arsenides: Synthesis, properties, and simulation. Computer Physics Communications, 50(3), 539-551.

[35] Boucetta, S. 2014, Theoretical study of elastic, mechanical and thermodynamic properties of MgRh intermetallic compound. Journal of Magnetic and Alloys. 2(1), 59–63.

[36] Martin, R.M. 2008, Electronic Structure Basic Theory and Practical Methods. New York, Cambridge university Press.

[37] Qia, L., Jina, Y., Zhaoa, Y., Yanga, X., Zhaoa, H., Han, P. 2015, The structural, elastic, electronic properties and Debye temperature of Ni_3Mo under pressure from first-principles. Journal of Alloys and Compounds, 621, 383–388.